Characterization of the Hanford 324 Building B Cell, Washington, USA - 11081

Walter S. Josephson, Worley Parsons Polestar
601 Williams Boulevard, Suite 4A, Richland WA 99352

ABSTRACT

The B hot cell in the 324 Building on the Department of Energy (DOE) Hanford site has been the subject of a significant cleanup effort. Exposure rate to activity modeling was used to assess the effectiveness of this effort, and to characterize B cell for demolition and disposal.

A detailed radiation survey of the interior of B cell was performed. In parallel, the physical structure of B cell, the radioactive source terms within, and the exposure rate measurement points were modeled using the Monte Carlo N-Particle (MCNP) code [1]. The MCNP model was used to calculate the relative contribution of each radioactive source to each exposure rate measurement point. The measured exposure rates and source contributions were entered into a matrix equation, and the least squares method was used to solve the equation for the activity of each radioactive source.

The matrix equation was also inverted to calculate the exposure rates predicted by the radioactive source activities. The predicted exposure rates were compared with the measured exposure rates to evaluate the quality of the least squares solution. The errors were found to be approximately normally distributed, with a mean of 0.5% and a standard deviation of 17%. The distribution of errors indicated that a high-quality solution was obtained.

INTRODUCTION

The 324 Building, built on the Hanford site 300 Area in 1966, played a key role in radiochemical and metallurgical research programs conducted by DOE. The B hot cell in the 324 Building was the site of high-level waste vitrification research, including research supporting the Hanford vitrification plant, and manufacture of glass logs for the Federal Republic of Germany (FRG). Normal cell operations, as well as spills, fires, and equipment failures over the years resulted in significant contamination in the cell.

B cell has been the subject of a multi-year cleanup and source term reduction effort to support facility demolition and waste disposal. As part of pre-demolition activities an assessment of the effectiveness of the cleanup effort was needed. Therefore, the decision was reached to re-characterize B cell, and compare the remaining source term with estimates prior the start of the clean-up effort. Exposure rate to activity modeling was selected for characterization of B cell due to the difficulty and high cost associated with a physical sampling and laboratory analysis approach.

EXPOSURE RATE MEASUREMENTS

The initial intent was to use an existing radiation survey performed within B cell to support cell characterization, primarily to avoid both the expense and equipment cycles associated with an extensive in-cell survey. However, as the cell characterization work progressed, a number of limitations associated with the existing survey became apparent.

- One of the functions of the existing survey was to evaluate the on-contact exposure rates from highly contaminated zones on the hot cell floor. While measuring the on-contact exposure rates, the probe became contaminated. Subsequently energizing the probe in one of the shielded ports resulted in an exposure rate reading of 50 Roentgen per hour above background.
- Baseline measurements for the probe were not taken, and the order of the exposure rate measurements was not recorded. Consequently, there was no way to determine which measurements were adversely affected by probe contamination, or how significant the effects may have been.
- There was concern that the radioactive contamination on the crane could be significant, and the location and orientation of the crane during the measurement process was not recorded. Therefore, the contribution from the crane could not be accurately modeled.

Ultimately, another survey was performed solely to support cell characterization. Procedures and data forms were revised to incorporate the additional requirements associated with exposure rate to activity modeling.

The characterization survey was performed using the Eberline RO-7 system [2], which features a hand-held instrument connected to a low-range, mid-range, or high-range probe. Each probe consists of an ion chamber sized to provide the desired sensitivity, as well as a matched pre-amplifier capable of transmitting the signal through up to 500 feet of cable. Use of the RO-7 system allowed the probes to reside in the hot cell while the instrument remained in the operating gallery.

The RO-7 probes were positioned within the cell using the B cell jib crane. Exposure rates high in the cell were measured with a mid-range probe and those low in the cell were measured using a high-range probe. The mid-range probe was carefully positioned within the cell to ensure that it did not over-range.

Clean RO-7 probes were introduced to the cell specifically for the characterization survey, and on-contact measurements were eliminated to minimize the potential for probe contamination. The exposure rates from the probes entering and leaving the cell were also recorded to evaluate the effects of probe contamination. The baseline measurements demonstrated that the survey was unaffected by probe contamination.

Exposure rates were generally taken on a horizontal grid beginning 30.48 cm (1 ft) from each wall and extending in a 182.88 cm (6 ft) by 152.4 cm (5 ft) pattern, and at elevations from 30.48 cm (1 foot) above the floor to the maximum height achievable by the crane. Certain grid points had to be moved, and others were not achievable, due to equipment in the cell. A total of 150 measurements were obtained during the characterization survey.

B CELL STRUCTURE

The physical structure of B cell was taken from Hanford construction drawings. The cell features shield walls of standard density concrete ranging from 173.16 cm (54 in) to 162.56 cm (64 in) in thickness, and a full stainless steel liner approximately 0.317 cm (1/8 in) thick. The floor of the cell is 15.24 cm (6 in) thick, and rests on compacted soil approximately 304.80 cm (10 ft) below grade.

The B cell structure includes a number of windows surrounded by high-density concrete, as well as manipulators, an overhead bridge crane with a rotating boom, carbon steel shield doors, an airlock, shielded pass-through ports of various sizes, and a HEPA filter bank along the north wall. Equipment associated with cell decontamination and routine operations is present on the floor. Some legacy items and failed equipment are also present on the floor.

The internal volume of the cell is a rectangle approximately 762.0 cm (25 ft) wide by 670.56 cm (22 ft) deep by 914.4 cm (30 ft) high. The floor of the cell is sloped to facilitate drainage, and along the east wall there is a 15.24 cm (6 in) wide sloped trench leading to a 60.96 cm by 60.96 cm (2 ft by 2 ft) sump in the northeast corner.

The construction details were simplified to minimize the MCNP modeling effort while retaining those features significant from an exposure rate to activity perspective. The windows and the associated high density concrete were replaced by standard concrete walls of uniform thickness. The pass-through ports and manipulators were omitted. The floor was modeled as a flat surface. The trench and sump were modeled as flat depressions in the floor. The equipment and legacy items on the floor were also omitted. The modeled details are shown in Figure 1.

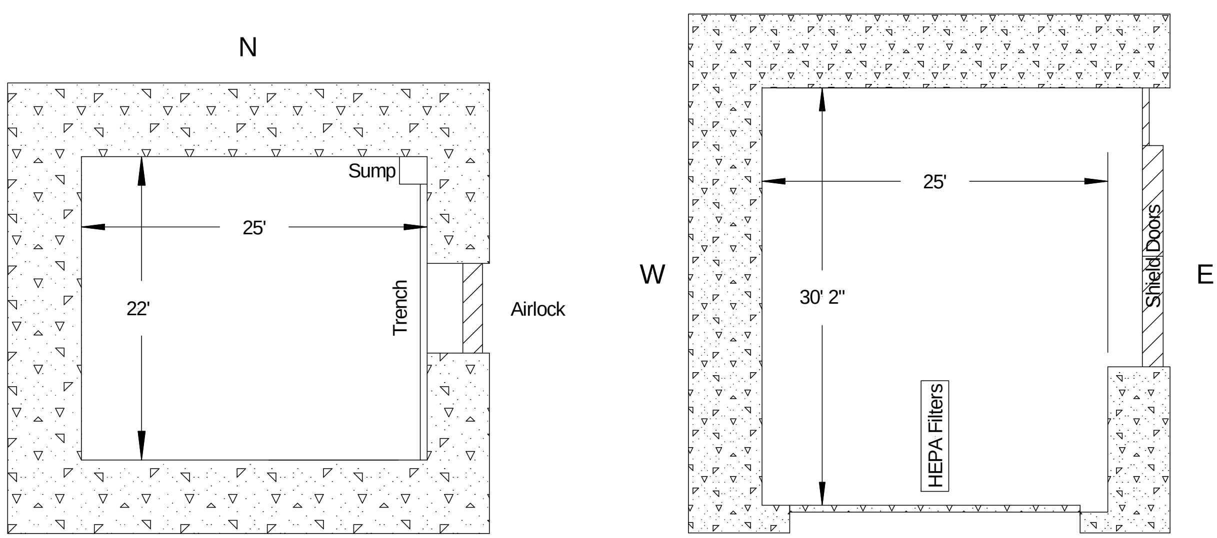

Figure 1. B Cell Structure

RADIOACTIVE SOURCE TERMS

The radioactive material in B cell was assumed uniform in composition. The isotopic distribution of the radioactive contamination on certain B cell equipment had been previously established by laboratory analysis of smears and physical samples. This composition was assumed to apply to the interior surfaces of B cell as well.

Uniform volume sources were used to represent the radioactive contamination on the crane and HEPA filters. The remaining radioactive material in B cell was assumed present as surface contamination. The internal surfaces of B cell were divided into 52 patches, and the radioactive contamination was assumed uniformly distributed within each patch. The size and location of each patch was subjectively determined based on the spatial exposure rate profile shown in the characterization survey.

PHOTON SPECTRUM

The established B cell isotopic distribution was modeled using the Oak Ridge Isotope Generation (ORIGEN) code [3] to calculate the photon spectrum. This approach was originally selected to ensure that contributions from bremsstrahlung would be included. However, bremsstrahlung contributions ultimately proved to be negligible.

The isotopic distribution relative to Cs-137 was normalized to a unit curie, then the normalized activities were converted to masses and entered into an ORIGEN input file. The ORIGEN input file was then executed to calculate the photon spectrum.

The predominant contributor to exposure rate proved to be Cs-137. Previous experience with ORIGEN spectra indicates that the 575 keV mean energy bin structure used by ORIGEN under-predicts the exposure rate from 662 keV photons from Cs-137 decay. The magnitude of the under-prediction is dependent on the type and thickness of shielding material between the source and measurement point, and can vary from essentially zero for air to slightly greater than 44% for 2.54 cm (1 in) of lead.

For B cell characterization, the mean energy of the 575 keV bin was shifted to 662 keV, and the photon rate for the bin was reduced to maintain the same energy rate. Although there was only air between the sources and measurement points, this approach was used to properly account for the contribution from backscatter off the cell walls.

TALLY CONVERSION FACTOR

MCNP tallies are reported in units of photon fluence per history, while the exposure rates measured using RO-7 probes are recorded in units of Roentgen per hour. Often MCNP calculations utilize fluence-to-dose factors to convert tally results to dose, and then assume that 0.01 Sv (1 rem) of dose is equivalent to one Roentgen of exposure. Use of this assumption introduces a bias whose magnitude is dependent on the source of the conversion factors used and the photon spectrum of the material in question.

The tally multiplier (FM) card provided in MCNP may be used to convert fluence tallies directly to Roentgen, thereby avoiding the bias introduced by using fluence-to-dose conversion factors. To assess the magnitude of the bias, a Cs-137 point source in air was modeled using MCNP. The exposure rate calculated directly by MCNP was compared to the dose rates calculated using several common sources of fluence-to-dose factors. The bias values are shown in Table I.

Table I. Fluence to Dose Bias

Fluence-Dose Factors	Bias
ANSI/ANS-6.1.1-1977 [4]	15.6%
ICRP 21 [5]	-1.6%
ANSI/ANS-6.1.1-1991 [6]	-7.0%
ICRP 51 [7]	-7.0%

For B cell characterization, the FM card approach was used to calculate exposure rate directly, thereby improving accuracy. The factor required by the FM card is derived as follows.

A tally (T) may be multiplied by the number of particle histories per unit time to convert from a per history basis to a per unit time basis. This may be done using the FM card constant, or by starting each particle with a weight (WGT) value equal to the particle rate per unit time. It is convenient to use the WGT parameter for this conversion because it is problem dependent, while the other contributors to the FM card constant are problem independent.

$$T \cdot WGT = \left(\frac{\text{particles}}{\text{cm}^2 \cdot \text{history}}\right) \cdot \left(\frac{\text{histories}}{\text{sec}}\right) = \frac{\text{particles}}{\text{cm}^2 \cdot \text{sec}} \qquad \text{(Eq. 1)}$$

A tally may be multiplied by the energy-dependent total reaction cross-section (σ_t) to convert to total reaction rate. Cross-sections in MCNP are microscopic quantities, and are recorded in units of barns. To obtain the macroscopic reaction rate in a material, the tally must also be multiplied by the atom density of the material (ρ_a). In MCNP, atom densities are expressed in units of barn-centimeters to simplify the multiplication.

$$T \cdot WGT \cdot \sigma_t \cdot \rho_a = \left(\frac{\text{particles}}{\text{cm}^2 \cdot \text{history}}\right) \cdot \left(\frac{\text{histories}}{\text{sec}}\right) \cdot (\text{b}) \cdot \left(\frac{\text{atoms}}{\text{b} \cdot \text{cm}}\right) = \frac{\text{reactions}}{\text{cm}^3 \cdot \text{sec}} \qquad \text{(Eq. 2)}$$

A reaction rate may be multiplied by the energy-dependent heating cross-section (σ_h) to convert to energy absorbed. Heating cross-sections are stored in units of MeV per collision. Since dosimetric quantities are stated in terms of energy absorbed per gram of material, the reaction rate may also be divided by the mass density (ρ_m) of the material in grams per cubic centimeter.

$$T \cdot WGT \cdot \sigma_t \cdot \sigma_h \cdot \left(\frac{\rho_a}{\rho_m}\right) = \left(\frac{\text{particles}}{\text{cm}^2 \cdot \text{history}}\right) \cdot \left(\frac{\text{histories}}{\text{sec}}\right) \cdot (\text{b}) \cdot \left(\frac{\text{MeV}}{\text{collision}}\right) \cdot \left(\frac{\text{atoms}}{\text{b} \cdot \text{cm}}\right) \cdot \left(\frac{\text{cm}^3}{\text{g}}\right) = \left(\frac{\text{MeV}}{\text{g} \cdot \text{sec}}\right) \qquad \text{(Eq. 3)}$$

The energy absorbed may be converted to Roentgen (R) if air is the absorbing material. The energy absorbed may be divided by the energy required to produce an ion pair in air (W) to convert to charge deposited. The charge deposited may be divided by the definition of a

Roentgen to convert to exposure in units of Roentgen. The time unit may also be converted to the more conventional hours. The value for the charge of an electron (e) was taken from CODATA 2006 [8], the value of W was taken from ICRU Report 31 [9], and the value of R was taken from NIST Special Publication 811 [10].

$$T \cdot WGT \cdot \sigma_t \cdot \sigma_h \cdot \left(\frac{\rho_a}{\rho_m \cdot W}\right) = \frac{\left(\frac{MeV}{g \cdot sec}\right) \cdot \left(\frac{cm^2}{b}\right) \cdot \left(\frac{e}{33.8\ eV}\right) \cdot \left(\frac{10^6\ eV}{MeV}\right) \cdot \left(\frac{1.602176487 \cdot 10^{-19}\ C}{e}\right) \cdot}{\left(\frac{R}{2.58 \cdot 10^{-4}\ C/kg}\right) \cdot \left(\frac{1000\ g}{kg}\right) \cdot \left(\frac{3600\ sec}{hr}\right)} = \frac{R}{hr} \qquad \text{(Eq.4)}$$

In the above equation, T is calculated by MCNP, WGT is supplied in the SDEF card, and the cross-sections are applied using the -5 and -6 reactions on the FM card. The remaining quantities constitute the constant C needed for the FM card to complete the conversion to Roentgen per hour.

$$C = \frac{\rho_a}{\rho_m \cdot W} \qquad \text{(Eq. 5)}$$

The quantity (ρ_a/ρ_m) is simply the Avogadro constant (N_{av}) divided by the formula mass of the material in question and converted to the appropriate units. The formula mass of the material may be calculated from the composition and density of the material, and the associated elemental masses. The formula mass calculation for air is shown in Table II. The elemental masses were taken from NUBASE 2003 [11], and the composition of air was taken from PNNL-15870 [12].

Table II. Formula Mass of Air

Air Composition		Element Mass	Formula Mass
Element	Mass Fraction	(g/mol)	(g/mol)
C	0.000124	12.010736	0.001489
N	0.755268	14.006743	10.578845
O	0.231781	15.999405	3.708358
Ar	0.012827	39.947677	0.512409
Total	1.000000		14.801101

Since atom densities in MCNP stated are in units of atoms per barn centimeter, and mass densities in MCNP are stated in units of grams per cubic centimeter, the quantity (ρ_a/ρ_m) must be stated in units of square centimeters per barn gram and not simply inverse grams. The constant C for the FM card necessary to calculate exposure in units of Roentgen per hour from a fluence tally is given by:

$$\frac{\rho_a}{\rho_m} = \frac{N_{av}}{FM} = \left(\frac{6.02214179 \cdot 10^{23}\ atoms}{mol}\right) \cdot \left(\frac{mol}{14.801101\, g}\right) \cdot \left(\frac{10^{-24}\ cm^2}{b}\right) = 4.069 \cdot 10^{-2}\ \frac{cm^2}{b \cdot g} \qquad \text{(Eq. 6)}$$

$$C = \frac{\left(4.069 \cdot 10^{-2}\ \frac{cm^2}{b \cdot g}\right) \cdot \left(\frac{1000\ g}{kg}\right) \cdot \left(\frac{e}{33.8\ eV}\right) \cdot \left(\frac{10^6 eV}{MeV}\right)}{\left(\frac{1.602176487 \cdot 10^{-19}\ C}{e}\right) \cdot \left(\frac{R}{2.58 \cdot 10^{-4}\ C/kg}\right) \cdot \left(\frac{3600\ sec}{hr}\right)} = 2.691 \cdot 10^{-6} \left(\frac{sec}{MeV}\right) \cdot \left(\frac{cm^2}{b}\right) \cdot \left(\frac{R}{hr}\right) \qquad \text{(Eq. 7)}$$

MCNP MODELS

MCNP models were constructed which incorporated all of the inputs generated in the preceding sections. To minimize wear on the crane, exposure rates were collected in a vertical string for a given crane position. Therefore, a separate MCNP input file was prepared for each x-y grid position in the characterization survey, and tallies were constructed in a vertical string in each MCNP input file.

Point detector tallies were constructed at each location in the survey plan, regardless of whether an exposure rate measurement was actually obtained at that location. Each point detector tally was modified with an FM card which multiplied the tally by the total and heating cross-sections of air and the constant developed above. Each tally was also modified with the SCX option of the FT card to implement source distribution flagging. Source distribution flagging forced the contribution from each source to each tally to be binned separately.

Each source was modeled as containing 0.037 TBq (1 Ci) of 324 B cell radioactive material. The WGT card was set to 54 times the total photon rate from 0.037 TBq (1 Ci) of 324 B cell radioactive material. All sources used the B cell photon spectrum. Particles were uniformly distributed in position in all sources. Importance and direction biasing was considered, but acceptable statistics proved to be readily obtained without biasing.

Because source distribution flagging was used to distinguish the contribution to each tally from each source, the PRDMP card was used to generate an MCTAL file for each case. Use of the MCTAL file option simplified the process of extracting data from the MCNP outputs.

The MCNP model was also executed with the concrete walls, liner, and other shielding structures replaced by air to evaluate the contribution from backscatter to the overall exposure rate. The backscatter contribution was approximately 10% near the walls and floor, and negligible near the center of the cell volume.

LEAST SQUARES SOLVER

The source activity to exposure rate factors (F) calculated by MCNP, the unknown radioactive source activities (S), and the characterization survey exposure rate measurements (ER) were cast as a matrix equation as follows.

$$F \cdot S = ER \qquad \text{(Eq. 8)}$$

Since there were 54 source activities and 150 exposure rate measurements, this equation was not square and could not simply be inverted to calculate the unknown source activities. Additional constraints were required to achieve a solution. For B cell characterization, the least squares methodology was used to supply the additional constraints. The least squares solution to Eq. 8 is given by:

$$S = \left(F^T \cdot F\right)^{-1} \cdot F^T \cdot ER \qquad \text{(Eq. 9)}$$

Because the least squares method involves a matrix inversion step, it is subject to the same numerical restrictions as matrix inversion. One of the major numerical restrictions is that if two of the simultaneous equations are the same within a multiplicative factor, then the matrix will be singular and not invertible. This situation can occur if two sources have the nearly the same contributions to all of the tally points. In the B Cell model, the sump, trench, and floor sources along the east wall fell into this category, as did the wall and floor sources in each of the four corners. To remedy this situation, one of the duplicate sources was retained, all of the remaining duplicate sources were constrained to zero, and the columns associated with the constrained sources were deleted from the Factors matrix.

A second numerical restriction is that if the activity of a source is small, it can lead to the calculation of unstable results. This is typically evidenced by pairs of large negative and positive results, which are generated by dividing by a number close to zero during the matrix operations. The results from the least squares solver was iteratively examined to identify those sources with very small contributions that were negatively affecting the performance of the solver.

During the iterative process, a total of 21 sources were constrained to zero, after which the least squares solver became numerically stable and produced physically realistic output for all of the remaining 33 sources. The contributions from the source patches associated with each internal surface were then summed to produce more meaningful output. The total activities were also multiplied by the isotopic distribution to produce isotopic activities for each surface. The results are shown in Table III.

Table III. Source Activities

Isotope	Floor (Ci)	Sump (Ci)	Trench (Ci)	Walls Below -9 ft (Ci)	Walls Above -9 ft (Ci)	Ceiling (Ci)
Co-60	2.52E-01	1.31E-01	4.06E-01	1.55E-02	2.12E-01	2.79E-02
Se-79	5.58E-04	2.91E-04	8.98E-04	3.44E-05	4.70E-04	6.19E-05
Sr-90	9.40E+02	4.90E+02	1.51E+03	5.78E+01	7.91E+02	1.04E+02
Y-90	9.40E+02	4.90E+02	1.51E+03	5.78E+01	7.91E+02	1.04E+02
Tc-99	1.86E-02	9.67E-03	2.99E-02	1.14E-03	1.56E-02	2.06E-03
Cs-137	1.75E+03	9.12E+02	2.82E+03	1.08E+02	1.47E+03	1.94E+02
Ba-137m	1.66E+03	8.63E+02	2.66E+03	1.02E+02	1.39E+03	1.84E+02
Eu-154	3.52E+00	1.83E+00	5.66E+00	2.16E-01	2.96E+00	3.90E-01
Eu-155	2.73E+00	1.42E+00	4.39E+00	1.68E-01	2.30E+00	3.03E-01
Pu-238	5.37E-01	2.80E-01	8.65E-01	3.31E-02	4.52E-01	5.96E-02
Pu-239	1.63E-01	8.52E-02	2.63E-01	1.01E-02	1.38E-01	1.81E-02
Pu-240	1.60E-01	8.36E-02	2.58E-01	9.86E-03	1.35E-01	1.78E-02
Pu-241	8.02E+00	4.18E+00	1.29E+01	4.93E-01	6.75E+00	8.89E-01

Pu-242	2.68E-04	1.40E-04	4.31E-04	1.65E-05	2.25E-04	2.97E-05
Am-241	2.36E+00	1.23E+00	3.80E+00	1.45E-01	1.99E+00	2.62E-01
Cm-243	1.51E-02	7.87E-03	2.43E-02	9.29E-04	1.27E-02	1.67E-03
Cm-244	1.04E+00	5.44E-01	1.68E+00	6.42E-02	8.78E-01	1.16E-01
Total	5.30E+03	2.77E+03	8.54E+03	3.26E+02	4.47E+03	5.88E+02

The activities shown above demonstrated that the B cell cleanup effort succeeded in removing approximately 75% of the residual activity.

UNCERTAINTY ANALYSIS

Once the source activities have been calculated, Eq. 8 may be used to calculate the exposure rates predicted by the source activities, and these exposure rates may be compared to the measured exposure rates in the characterization survey. The results of this comparison are shown in Figure 2.

The differences were found to be approximately normally distributed, with a mean of 0.5% and a standard deviation of 17%. The large number of differences in the +5% bin indicate that the calculated source activities are biased slightly high.

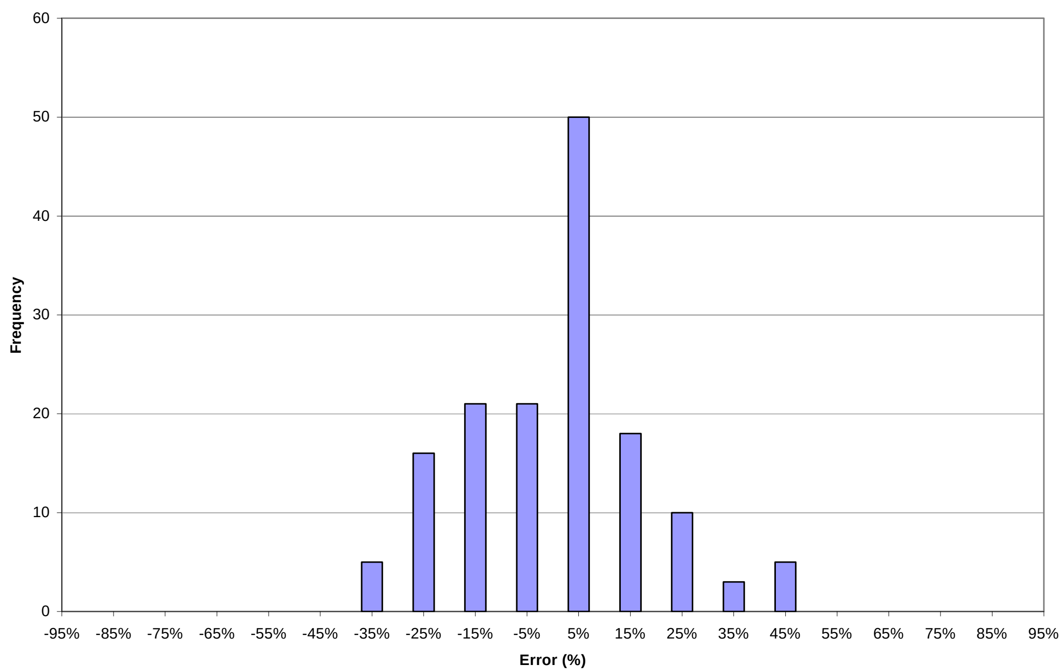

Figure 2. Error Histogram

The level of agreement between the model and the measured dose rates shown in Figure 2 is notably better than typical for exposure rate to activity modeling, particularly for a scenario as challenging as B cell. Some sources of uncertainty and reasons why their effects may have been less than expected are discussed below.

- Field dose rate instruments are somewhat sensitive to ambient temperature, pressure, and humidity. Environmental effects are minimized by:
    - The RO-7 instrument was maintained in the relatively controlled conditions of the operating gallery, which minimizes the sensitivity to variations in temperature.
    - B cell is maintained at a negative pressure of only a fraction of an inch of mercury, which along with the 120 m (400 ft) elevation of the Hanford 300 area minimizes the sensitivity to variations in atmospheric pressure.
    - The RO-7 ion chamber vents to ambient via a desiccant pack, which minimizes the sensitivity to variations in humidity.
    - The SI definition of the Roentgen used in the MCNP model assumes dry air at 15 ºC and one atmosphere, which approximate the conditions prevalent in B cell when the exposure rates were measured.
- The RO-7 instrument is calibrated to within ± 20% [2], and is also subject to drift after calibration. Together these constitute randomly distributed measurement uncertainties. The effects of these uncertainties are minimized by the use of a large number of exposure rate measurements, which tend to average out random phenomena.
- The actual composition of the radioactive material in B cell is uncertain, and may vary with location. The effect of this uncertainty is minimized due to the preponderance of Cs-137 in the photon spectrum.
- The actual distribution of radioactive material in B cell is uncertain, and undoubtedly includes more structure than is reproducible by the limited number of sources in the model. The effect of this uncertainty is minimized by the use of a large number of exposure rate measurements, most of which are well removed from the radioactive material.

REFERENCES

1. "MCNP - A General Monte Carlo N-Particle Transport Code, Version 5," LA-UR-03-1987, Los Alamos National Laboratory (2005).
2. "Radiation Protection Instrument Manual," PNNL-14135, Revision 1, Pacific Northwest National Laboratory (2009).
3. "A User's Manual for the ORIGEN2 Computer Code," ORNL/TM-7175, Oak Ridge National Laboratory (1980).
4. "Neutron and Gamma-Ray Flux-to-Dose-Rate Factors," ANSI/ANS-6.1.1-1977, American Nuclear Society (1977).
5. "Data for Protection Against Ionizing Radiation from External Sources: Supplement to ICRP Publication 15," ICRP 21, International Commission on Radiological Protection (1971).
6. "Neutron and Gamma-Ray Fluence-to-Dose Factors," ANSI/ANS-6.1.1-1991, American Nuclear Society (1991).
7. "Data for Use in Protection against External Radiation," ICRP 51, International Commission on Radiological Protection (1987).
8. "CODATA Internationally Recommended Values of the Fundamental Physical Constants," Reviews of Modern Physics, vol. 80, page 633-730 (2006).
9. "Average Energy Required to Produce an Ion Pair," ICRU Report 31, International Commission on Radiation Units and Measurements (1979).

10. “Guide for the use of the International System of Units (SI),” Special Publication 811, National Institute for Science and Technology (2008).
11. “The NUBASE 2003 Evaluation of Nuclear and Decay Properties,” Nuclear Physics A, vol. 729, page 3-128 (2003).
12. “Compendium of Material Composition Data for Radiation Transport Modeling,” PNNL-15870, Pacific Northwest National Laboratory (2006).